J. Org. Chem. 1990, 55, 3582–3593

A Theoretical Study on Ketene–Olefin Cycloadditions. 1. Intermolecular Reactions

Eduard Valentí, Miquel A. Pericàs,* and Albert Moyano*

Departament de Química Orgànica, Universitat de Barcelona, Martí i Franquès 1-11.08028-Barcelona, Spain

Received October 23, 1989

The cycloaddition reaction between ketenes and olefins, leading to cyclobutanones, has been theoretically studied by means of the semiempirical AM1 methodology. A representative set of 7 differently substituted ketenes and 3 olefins has been selected, and 50 transition states, corresponding to different ketene–olefin approach geometries, have been located and characterized. The reaction is seen to be concerted in all but in two cases, taking place through twisted transition states with small charge transfer from the olefin to the ketene. A reaction analysis by correlation of localized molecular orbitals shows that the reaction mechanism corresponds to the $[_{\pi}2_{s} + (_{\pi}2_{s} + _{\pi}2_{s})]$ description, rather to the $[_{\pi}2_{s} + _{\pi}2_{a}]$ one. The regioselectivity and the stereoselectivity of the reaction are correctly predicted by the calculations and are analyzed in terms of electronic and steric effects of the substituents on the reacting ketene and olefin partners.

Introduction

The [2 + 2] cycloaddition between ketenes and alkenes leading to cyclobutanones (Scheme I) constitutes a process of paramount importance from the synthetic point of view.[1] The interest in this subject continues unabated, as exemplified by recent developments of the reaction in the fields of intramolecular multiannelation processes[2] and of enantioselective ring construction.[3]

In order to explain the high degree of peri-, regio- and stereoselectivity shown by the reaction, a great number of kinetic studies have been devoted to it.[1,4-8] With the exception of ketene cycloaddition to enamines,[9] the available experimental evidence points toward a concerted mechanism involving a transition state with some charge separation.

On the other hand, the number of theoretical studies on this reaction is very small. Woodward and Hoffmann analyzed the ketene–alkene cycloaddition in terms of a concerted $[_{\pi}2_{s} + _{\pi}2_{a}]$ reaction in which the olefinic portion of the ketene acted as the antarafacial component.[10] The overlap inefficiency of this approach, requiring a perpendicular confrontation of the alkene and the ketene, was supposedly compensated by means of secondary orbital interactions betwen the HOMO of the alkene and the low-lying antibonding $\pi^*_{C=O}$ orbital of the ketene (Figure 1a).

Scheme I

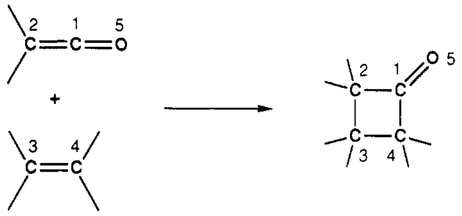

Since this analysis provided a rationale for the remarkable stereochemical issues of the reaction (syn stereospecificity with respect to the alkene and high stereoselectivity with respect to the ketene which places its larger substituent in the more hindered face of the cyclobutanone), the Woodward–Hoffmann transition state has been generally accepted without further criticism. An alternative view[4,11] has been proposed of the reaction in terms of two basic processes which, by taking place in a simultaneous way, lead to a concerted process: A nucleophilic attack of one carbon of the alkene to the ketene carbonyl, and a subsequent attack of the ketene terminal carbon to the other carbon of the alkene (Figures 1b and 1c). A geometric analysis of the resulting transition state shows that avoidance of repulsion between the largest substituents on the ketene and the alkene results in the formation of the less stable cyclobutanone. This alternative mechanism, which has been called $[_{\pi}2_{s} + (_{\pi}2_{s} + _{\pi}2_{s})]$, is clearly superior to the $[_{\pi}2_{s} + _{\pi}2_{a}]$ one in the case of the cycloaddition reactions of allenes with alkenes[12] and of dichloroketene with monosubstituted benzaldehydes.[13]

In 1985, Burke has reported the results of ab initio, minimal basis set, calculations (including configuration interaction) for the cycloaddition of ketene to ethene.[14] The lowest energy reaction path found in this study is a concerted, nonsynchronous one, with a transition state where a single bond between the carbonyl carbon of ketene

---

[1] For some recent reviews, see: (a) Ghosez, L.; O'Donnell, M. J. In *pericyclic Reactions*; Marchand, A. P., Lehr, R. E., Eds.; Academic Press: New York, 1977; Vol. II, pp 79–140. (b) Ghosez, L. In *Stereoselective Synthesis of Natural Products*; Bartmann, W., Winterfeldt, E., Eds.; Excerpta Medica: Amsterdam-Oxford, 1979; pp 93–105. (c) Brady, W. T. *Tetrahedron* **1981**, *37*, 2949. (d) Holder, R. W. *J. Chem. Ed.* **1976**, *53*, 81. (e) Brady, W. T. In *The Chemistry of Ketenes and Allenes and Related Compounds*; Patai, S., Ed.; Wiley: New York, 1980; pp 279–413.

[2] (a) Markó, I.; Ronsmans, B.; Hesbain-Frisque, A. M.; Dumas, S.; Ghosez, L.; Ernst, B.; Greuter, H. *J. Am. Chem. Soc.* **1985**, *107*, 2192. (b) Snider, B. B.; Hui, R. A. H. F.; Kulkarni, Y. S. *J. Am. Chem. Soc.* **1985**, *107*, 2194. (c) Kulkarni, Y. S.; Niwa, M.; Ron, E.; Snider, B. B. *J. Org. Chem.* **1987**, *52*, 1568. (d) Corey, E. J.; Kang, M.-C.; Desai, M. C.; Ghosh, A. K.; Houpis, I. N. *J. Am. Chem. Soc.* **1988**, *110*, 649. (e) De Mesmaeker, A.; Veenstra, S. J.; Ernst, B. *Tetrahedron Lett.* **1988**, *29*, 459. (f) Snider, B. B.; Niwa, M. *Tetrahedron Lett.* **1988**, *29*, 3175. (g) Snider, B. B. *Chem. Rev.* **1988**, *88*, 793.

[3] (a) Greene, A. E.; Charbonnier, F. *Tetrahedron Lett.* **1985**, *26*, 5525. (b) Fráter, G.; Müller, U.; Günther, W. *Helv. Chim. Acta* **1986**, *69*, 1858. (c) Greene, A. E.; Charbonnier, F.; Luche, M.-J.; Moyano, A. *J. Am. Chem. Soc.* **1987**, *109*, 4752.

[4] Baldwin, J. E.; Kapecki, J. A. *J. Am. Chem. Soc.* **1970**, *92*, 4868, 4874.

[5] Huisgen, R.; Feiler, L. A.; Otto, P. *Tetrahedron Lett.* **1968**, 4485.

[6] Katz, J.; Dessau, R. *J. Am. Chem. Soc.* **1969**, *85*, 2172.

[7] Egger, K. W. *J. Am. Chem. Soc.* **1973**, *95*, 1745.

[8] Huisgen, R.; Feiler, L. A. *Chem. Ber.* **1969**, *102*, 3444.

[9] (a) Hoch, H.; Hunig, S. *Chem. Ber.* **1972**, *105*, 2660. (b) Feiler, L. A.; Huisgen, R. *Chem. Ber.* **1969**, *102*, 3428. (c) Huisgen, R.; Otto, P. *J. Am. Chem. Soc.* **1969**, *91*, 5922. (d) Otto, P.; Feiler, L. A.; Huisgen, R. *Angew. Chem., Int. Ed. Engl.* **1969**, *7*, 737.

[10] Woodward, R. B.; Hoffmann, R. *The Conservation of Orbital Symmetry*; Verlag Chemie: Weinheim, 1970; p 68.

[11] Zimmerman, H. E. *Pericyclic Reactions*; Marchand, A. P., Lehr, R. E., Eds.; Academic Press: New York, 1977; Vol. I, pp 77–78.

[12] Pasto, D. J. *J. Am. Chem. Soc.* **1979**, *101*, 37.

[13] Krabbenhoft, H. O. *J. Org. Chem.* **1978**, *43*, 1305.

[14] Burke, L. A. *J. Org. Chem.* **1985**, *50*, 3149.

0022-3263/90/1955-3582$02.50/0 © 1990 American Chemical Society

Chart I

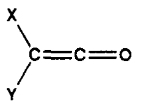

1

- a X = Y = H
- b X = H, Y = Cl
- c X = Y = Cl
- d X = H, Y = CH_3
- e X = H, Y = OCH_3
- f X = H, Y = $CH{=}CH_2$
- g X = H, Y = C_6H_5

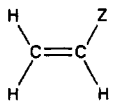

2

- a Z = H
- b Z = CH_3
- c Z = OCH_3

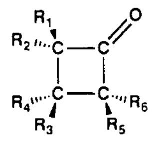

3

cyclobutanone	R_1	R_2	R_3	R_4	R_5	R_6
3a	H	H	H	H	H	H
3b	Cl	H	H	H	H	H
3c	Cl	Cl	H	H	H	H
3d	CH_3O	H	H	H	H	H
3e	CH_3	H	H	H	H	H
3f	$CH_2{=}CH$	H	H	H	H	H
3g	C_6H_5	H	H	H	H	H
3h	H	H	CH_3	H	H	H
3i	H	H	CH_3O	H	H	H
3j	Cl	Cl	CH_3	H	H	H
3k	Cl	Cl	H	H	CH_3	H
3l	Cl	Cl	CH_3O	H	H	H
3m	Cl	Cl	H	H	CH_3O	H
3n	Cl	H	CH_3	H	H	H
3o	CH_3	H	CH_3	H	H	H
3p	Cl	H	CH_3O	H	H	H
3q	CH_3	H	CH_3O	H	H	H
3r	Cl	H	H	CH_3	H	H
3s	CH_3	H	H	CH_3	H	H
3t	Cl	H	H	CH_3O	H	H
3u	CH_3	H	H	CH_3O	H	H
3v	Cl	H	H	H	CH_3	H
3w	CH_3	H	H	H	CH_3	H
3x	Cl	H	H	H	CH_3O	H
3y	CH_3	H	H	H	CH_3O	H
3z	Cl	H	H	H	H	CH_3
3aa	CH_3	H	H	H	H	CH_3
3ab	Cl	H	H	H	H	CH_3O
3ac	CH_3	H	H	H	H	CH_3O

and one carbon of ethene is almost completely formed, while the terminal methylene groups are only slightly bonded. Although this is not stated by the author, this mechanism corresponds to the $[{}_{\pi}2_{s} + ({}_{\pi}2_{s} + {}_{\pi}2_{s})]$ one. The calculated activation energy (according to single point calculations at the MP4/6-31G level on STO-3G partially optimized geometries) is 24 kcal mol^{-1} higher than the experimental value. The reaction paths corresponding to the $[{}_{\pi}2_{s} + {}_{\pi}2_{a}]$ and $[{}_{\pi}2_{s} + {}_{\pi}2_{s}]$ mechanisms are predicted to have activation energies 19 and 29 kcal mol^{-1} higher, respectively, than the $[{}_{\pi}2_{s} + ({}_{\pi}2_{s} + {}_{\pi}2_{s})]$ one. Since no complete geometry optimizations nor force constants calculations were performed, the results of this study, although very interesting, should be regarded as provisory. Very recently, Bernardi, Robb, and co-workers,[15] using complete active space self-consistent field (CASSCF) calculations,[16] have shown that the critical point associated with the $[{}_{\pi}2_{s} + {}_{\pi}2_{a}]$ approach between ketene and ethene is not a true transition state, since its force constant matrix has two negative eigenvalues. In any case, a theoretical study involving substituted ketenes and/or alkenes, more directly related to cases of actual synthetic interest, is still lacking. It should be noted here that other recent theoretical studies on ketene reactivity have been devoted to the closely related but clearly different subjects of ketene dimerization[17] and of the cycloaddition of ketene radical cation with ethene.[18]

Moreover, from the experimental point of view, a clear understanding of substituent effects in the reaction would be very important. For instance, intramolecular ketene–olefin cycloadditions are known to proceed with synthetically useful yields only with alkoxy-, vinyl-, or aryl-substituted ketenes, but the precise role of the ketene substituents (i.e., if they accelerate the cycloaddition either by energetic or entropic factors, or if they simply diminish

---

[15] Bernardi, F.; Bottoni, A.; Olivucci, M.; Robb, M. A.; Schlegel, H. B.; Tonachini, G. *J. Am. Chem. Soc.* **1988**, *110*, 5993.

[16] (a) Hegarty, D.; Robb, M. A. *Mol. Phys.* **1979**, *38*, 1795. (b) Robb, M. A.; Eado, R. H. A. *NATO Adv. Study Inst. Ser., Ser. C* **1981**, *67*, 21. (c) Schlegel, H. B.; Robb, M. A. *Chem. Phys. Lett.* **1982**, *93*, 43.

[17] Xiaoyuan, F.; Decai, F.; Yambo, D. *J. Mol. Struct.* (*Theochem*) **1988**, *167*, 349.

[18] Heinrich, N.; Koch, W.; Morrow, J. C.; Schwarz, H. *J. Am. Chem. Soc.* **1988**, *110*, 6332.

Table I. Relevant Geometrical Parameters[a,b] in the AM1 Optimized Transition States, Enthalpies of Activation[c] ($\Delta H^{\ddagger}$), and Enthalpies of Reaction[c] (ΔH_r) for the Cycloaddition of Symmetrically Substituted Ketenes with Ethene

ketene	olefin	cyclobutanone	r_{12}	r_{23}	r_{34}	r_{41}	r_{15}	$\Delta H^{\ddagger}$	ΔH_r
1a	**2a**	**3a**	1.377	2.474	1.404	1.714	1.229	39.8	−35.3
1a	**2a**	**3a**[d]	1.378	2.671	1.398	1.705	1.232	48.0	−19.9
1c	**2a**	**3c**	1.404	2.741	1.411	1.634	1.234	33.1	−29.9

[a] Atom numbering as defined in Scheme I. [b] r_{xy} are the distances in angstroms between atoms x and y. [c] At 298 K, in kcal mol^{-1}. [d] 3 × 3 CI results.

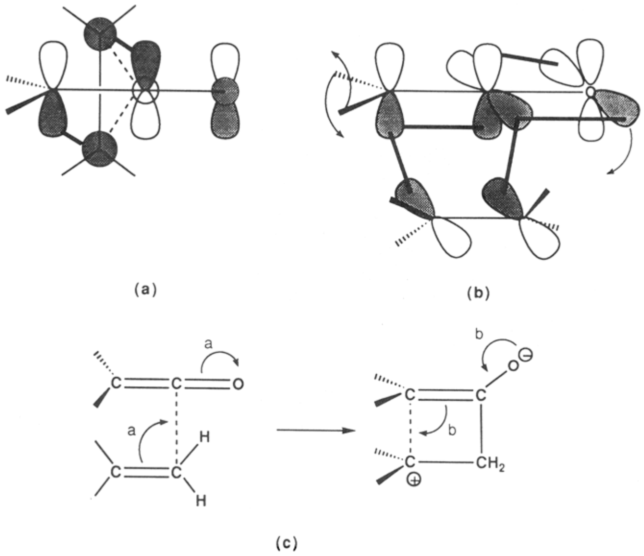

Figure 1. Mechanistic pictures of the ketene olefin cycloaddition: (a) orbital interactions in the $[{}_{\pi}2_{s} + {}_{\pi}2_{a}]$ mechanism; (b) orbital interactions in the $[{}_{\pi}2_{s} + ({}_{\pi}2_{s} + {}_{\pi}2_{s})]$ mechanism; (c) π-electron movement associated to the $[{}_{\pi}2_{s} + ({}_{\pi}2_{s} + {}_{\pi}2_{s})]$ mechanism.

the rate of competing dimerization or polymerization reactions), is not fully understood.[2] In the present paper, we address theoretically for the first time the effect of both ketene and olefin substituents in the cycloaddition process with regard to the energetic, regioselective, and stereoselective aspects of the reaction in its intermolecular version. The corresponding issues of the intramolecular ketene–olefin cycloaddition will be discussed in a separate paper.[19]

We have selected for the present study the sets of ketenes, **1a–g**, and of alkenes, **2a–c**, and we have investigated their cycloaddition leading to cyclobutanones **3a–ac** (Chart I).

Theoretical Procedure

The calculations reported in the present study were performed with the semiempirical AM1 method,[20] as implemented in a locally modified version of the MOPAC package of programs,[21] which includes the AM1 hamiltonian. The standard Restricted Hartree Fock (RHF) version was used throughout, since: (a) the 55 × 55 configuration interaction (CI) calculations of Burke[14] showed that the ground-state self-consistent field (SCF) configuration predominates in the expansion, and (b) either 3 × 3 CI RHF or two-configuration self-consistent field (TCSCF)[22] AM1 calculations performed for the cycloaddition between ketene (**1a**) and ethene (**2a**) corroborated this result. Equilibrium geometries for reactants and products were determined by minimization of the energy with respect to all geometrical parameters using the DFP algorithm.[23] Transition states (TSs) were generally located by means of the reaction coordinate method, starting from the cyclobutanone; in some instances, they were obtained by pertinent substitution on other, previously located, transition states and further optimization with the NLLSQ algorithm.[24] All transition states were refined by minimization of the gradient norm of the energy[25] and characterized by establishing that the Hessian (force constant) matrix had one and only one negative eigenvalue.[25] Transition structures containing the methoxy group (either on the ketene or the olefin fragments) were located and characterized for all conformations of this substituent. The given data refer always to the most stable conformer. Allowance for geometrical relaxation from the transition states after small geometrical distortions led in all cases to the starting cyclobutanone and to the corresponding ketene and olefin fragments (see below for the cycloaddition of **1c** with **2c** leading to **3l**).

In order to get a deeper insight into the electronic reorganization taking place during the reaction, as we have discussed elsewhere,[26,27] the localized molecular orbitals (LMO's) of reactants, products and transition states were obtained with the localization procedure implemented in MOPAC, which essentially consists in a reformulation[28] of the Von Niessen density-localization criterion.[29] The progress of the reactions was also followed by means of the bond index (B_{xy})[30] between atoms x and y, as defined by eq 1, where $P_{\gamma\delta}$ are the elements of the density matrix and the subscripts γ and δ refer to atomic orbitals centered at atoms x and y, respectively.

$$B_{xy} = \sum\sum P_{\gamma\delta}^{2} \tag{1}$$

The bond index analysis[27] of the reactions was performed by examination of the relative variation of bond index at the transition state (δB_i)[27] for every bond (i) involved in the reaction as defined by eq 2, where the subscripts R, TS and P refer to reactants, transition state, and product, respectively.

$$\delta B_i = (B_i^{TS} - B_i^{R})/(B_i^{P} - B_i^{R}) \tag{2}$$

The degree of advancement of the transition state along the reaction coordinate can be evaluated in a simple way as δB_{av},[27] i.e., the average value of δB_i, whereas the absolute asynchronicity of the reaction

---

(19) Valentí, E.; Pericàs, M. A.; Moyano, A. To be submitted for publication.

(20) Dewar, M. J. S.; Zoebisch, E. G.; Healy, E. F.; Stewart, J. J. P. *J. Am. Chem. Soc.* **1985**, *107*, 3902.

(21) IBM/CMS Version QCPE 486; Olivella, S. *QCPE Bull.* **1984**, *4*, 10.

(22) Bofill, J. M.; Gômez, J.; Olivella, S. *J. Mol. Struct.* (*Theochem*) **1988**, *163*, 285.

(23) (a) Fletcher, R.; Powell, M. J. D. *Comput. J.* **1963**, *6*, 163. (b) Davidon, W. C. *Comput. J.* **1968**, *11*, 406.

(24) Bartels, R. H. Report CNA-44, 1972; University of Texas Center for Numerical Analysis.

(25) McIver, J. W.; Komornicki, A. *J. Am. Chem. Soc.* **1972**, *94*, 2625.

(26) Moyano, A.; Pericàs, M. A.; Serratosa, F.; Valentí, E. *J. Org. Chem.* **1987**, *52*, 5532.

(27) Moyano, A.; Pericàs, M. A.; Valentí, E. *J. Org. Chem.* **1989**, *54*, 573.

(28) (a) Paniagua, J. C.; Moyano, A.; Tel, L. M. *Int. J. Quantum Chem.* **1984**, *26*, 383. (b) Perkins, P. G.; Stewart, J. J. P. *J. Chem. Soc., Faraday Trans. 2* **1982**, *78*, 285.

(29) Von Niessen, W. *J. Chem. Phys.* **1972**, *56*, 4290.

(30) Wiberg, K. B. *Tetrahedron* **1968**, *24*, 1083.

Table II. Evolution of Relevant Bond Indices[a,b] and Net Atomic Charges[a] Along the Reaction Coordinate for the Cycloaddition of Ketene with Ethene

reaction stage	B_{12}	B_{23}	B_{34}	B_{41}	B_{51}	q_1	q_2	q_3	q_4	q_5
ketene + ethene	1.747	0.000	2.002	0.000	2.015	0.256	−0.441	−0.218	−0.218	−0.167
transition state	1.391	0.312	1.358	0.540	1.764	0.249	−0.401	−0.029	−0.281	−0.328
cyclobutanone	0.919	0.986	0.986	0.919	1.939	0.229	−0.231	−0.168	−0.231	−0.261
δB_i[c]	0.430	0.316	0.634	0.588						

[a] Atom numbering as defined in Scheme I. [b] According to eq 1. [c] According to eq 2.

(A)[27] is given by eq 3, where n is the number of bonds directly involved in the reaction.

$$A = 1/(2n - 2)\sum(|\delta B_i - \delta B_{av}|/\delta B_{av}) \qquad (3)$$

Results and Discussion

In all the studied cases except in the reaction of **1c** with **2c** leading to **3l**, the [2 + 2] cycloaddition between ketenes and olefins is predicted to be a concerted process taking place through a twisted transition state with small charge separation. Since the symmetry characteristics of the reacting ketene and olefin determine the number of possible interaction modes between them, the studied processes have been classed into four general types of increasing complexity which will be discussed successively.

1. Symmetrically Substituted Ketenes (1a and 1c) with Ethene (2a). The cycloaddition between symmetrically substituted ketenes and ethene (or a completely symmetrical tetrasubstituted derivative) represents the simplest case of the reaction, since only one interaction mode of the reactants can be in principle expected. The relevant geometrical parameters of the transition states in the considered reactions are summarized in Table I, together with the corresponding activation and reaction enthalpies.

In the first place, in order to ascertain if the AM1 method gave results in accordance with those obtained by Burke[14] and with experimental evidence, we studied the reaction between the unsubstituted partners **1a** and **2a**, leading to cyclobutanone (**3a**), at the RHF level. Starting from **3a**, and using a combination of the dihedral angle and the distance between the ketene and ethene moieties of the molecule as the reaction coordinate, a transition state (shown in Figure 2) was located.

The geometrical characteristics of this structure (Table I, first entry) show that it is essentially identical with the lowest energy critical point found by Burke along what he called the "two-step" path (r_{14} = 1.80 Å, r_{23} = 2.75 Å).[14] From the geometrical point of view, such a TS would appear as substantially asynchronous, since the 1–4 distance (1.71 Å) is substantially shorter than the 2–3 one (2.47 Å); we will see later how the bond index analysis shows that, in fact, the asynchronicity is considerably lower. The four-membered ring is considerably twisted (the dihedral angle between the planes defined by atoms 1–2–3 and 1–4–3 has a value of 53°), and the terminal CH_2 group of the ketene is almost perpendicular to the "open" CH_2 group (i.e., that corresponding to C_3) of ethene (the value of the dihedral angle is of ca. 90°).

The calculated enthalpy of activation (39.8 kcal mol^{-1}) is in much better agreement with the estimated experimental value (ca. 32 kcal mol^{-1}, obtained from the experimental activation energy of the thermal decomposition of cyclobutanone[31] and from the estimated heat of formation for cyclobutanone[32] and the experimentally known heats of formation of ketene[33] and ethene[33]) than the value calculated by Burke (58 kcal mol^{-1}).[14]

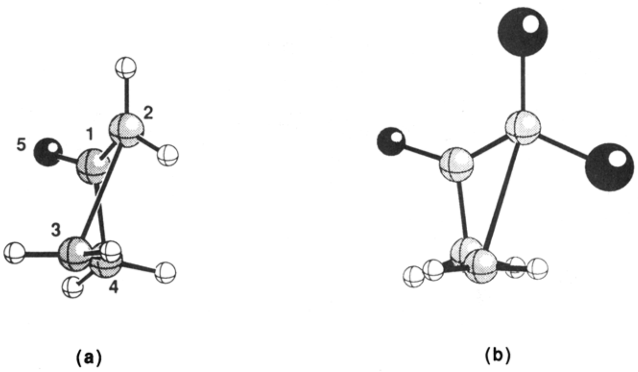

Figure 2. Computer plot of the calculated transition states for the cycloaddition of (a) ketene (**1a**) with ethene (**2a**), and (b) dichloroketene (**1c**) with ethene (**2a**).

Other approach geometries were also investigated at the RHF level. For the $[2\pi_s + 2\pi_s]$ approach which, according to Burke,[14] does not seem to be symmetry forbidden, a stationary point was located with an energy 12.9 kcal mol^{-1} higher than the previously located TS. This structure, however, does not correspond to a true transition state since its Hessian matrix has two negative eigenvalues.

As stated before, we have performed RHF 3 × 3 CI and TCSCF calculations on this system, in order to investigate the existence of alternative pathways taking place through biradicaloid species. The results of the 3 × 3 CI study based on molecular orbitals given by the RHF method are summarized in the second entry of Table I. Whereas the geometric characteristics of the TS are very similar to those of the monoconfigurational one, the energetic description of the reaction is worse. Since the weight of the ground-state configuration turns out to be largely (96%) predominant, the 3 × 3 CI calculations indicate that the process can be properly described by a monoconfigurational RHF treatment. On the other hand, when the potential energy hypersurface was explored by means of AM1–TCSCF calculations, no transition structure could be located; however, a single-point calculation on the RHF refined TS geometry indicated some diradical character. Thus, two configurations contribute to the description of these species (a^2, 0.907; b^2, 0.417), but the ground-state one (a^2) largely predominates (83%). It turns out that RHF calculations can afford a sufficiently accurate description of the cycloaddition of ketene (**1a**) with ethene (**2a**) for the purposes of the present study. Accordingly, we will exclusively refer in the subsequent discussion to the results of monoconfigurational RHF calculations.

The evolution of relevant net atomic charges (calculated from Mulliken population analysis within the zero differential overlap (ZDO) approximation) and bond indices along the reaction coordinate is given in Table II.

It can be seen that some electron density (0.23 e) has been transferred from the olefin to the ketene fragment

---

(31) Das, M. N.; Kern, F.; Coyle, T. D.; Walters, W. D. *J. Am. Chem. Soc.* **1954**, *76*, 6271.

(32) McGee, T. H.; Schleifer, A. *J. Phys. Chem.* **1972**, *76*, 963.

(33) Pedley, J. B.; Naylor, R. D.; Kirby, S. P. *Thermochemical Data of Organic Compounds*, 2nd ed.; Chapman and Hall: London, 1986.

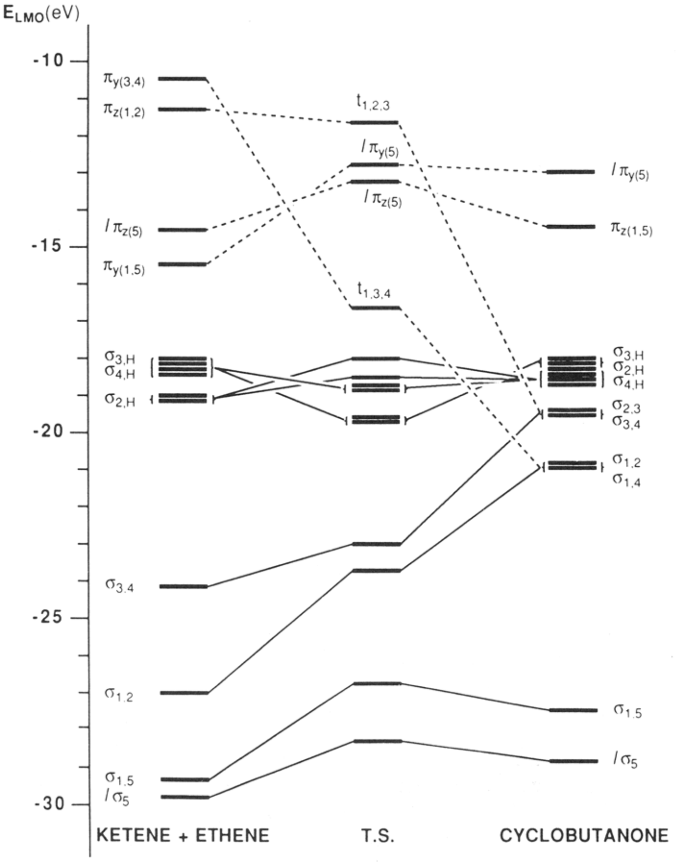

Figure 3. Correlation diagram of the localized molecular orbitals in the cycloaddition of ketene (**1a**) with ethene (**2a**). Atom numbering, as defined in Scheme I, is retained for the transition state. The meaning of the labels is as follows: σ and π refer to the local symmetry of localized bicentric orbitals, $l\sigma$ and $l\pi$ refer to localized monocentric orbitals, and t refers to localized tricentric orbitals. The broken lines connect the orbitals corresponding to the bonds which are made or broken in the reaction.

in the TS and some charge separation arises between the C_3 and O_5 atoms relative to reactants and product. The slight zwitterionic character of the transition state had been anticipated by several experimental results: the existence of linear Hammett plots,[4] rate enhancements in polar solvents,[5] and the regioselectivity of the cycloaddition in the case of substituted alkenes[1] (see below). The bond index analysis (restricted to the four bonds which are "broken" or "formed" in the overall process, since the C_1–O_5 bond index, although somewhat diminished in the TS, remains essentially the same in reactants and product), gives a degree of advancement of the transition state (δB_{av}) value of 0.492 (i.e., a TS "halfway" alone the reaction coordinate) and an asynchronicity A value of 7.9%, so that the reaction appears to be considerably more synchronous than anticipated by simple inspection of bond distances. In effect, although the C_2–C_3 distance at the TS is of 2.47 Å, a substantial bond index between C_2 and C_3 (0.312) is already present.

In order to analyze the electronic changes taking place along the reaction path in terms of the "movement" of electron pairs, the calculated LMO's for reactants (**1a** and **2a**), transition state, and cyclobutanone (**3a**) were classified according to their local symmetry (σ or π) and nature (lone pair, bicentric, or tricentric), and a correlation diagram was set up following the evolution of the LMO's from reactants to product through the transition state (Figure 3).

Since the reaction involves two perpendicular π systems at ketene, in order to facilitate the discussion we start from a ketene molecule lying on the xy plane, with an ethene molecule approaching perpendicularly to it along the y axis (see Figure 4).

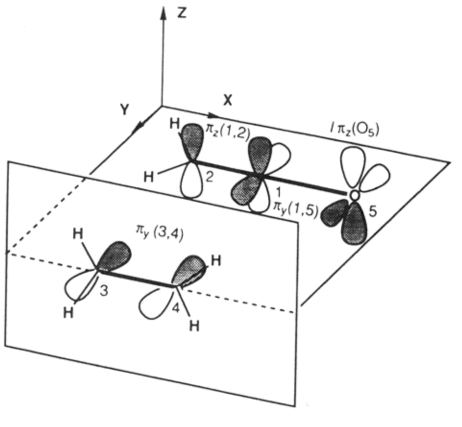

Figure 4. Schematic representation of the localized molecular orbitals of ethene (**a**) and ketene (**1a**) relevant to the cycloaddition process.

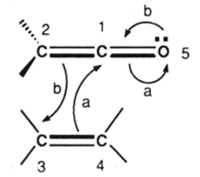

Figure 5. Schematic representation of the electronic reorganization in the cycloaddition of ketene (**1a**) with ethene (**2a**). Compare with Figure 1c.

In this way, the identity of the calculated transition state with the $[_\pi 2_s + (_\pi 2_s + _\pi 2_s)]$ one is easily visualized by inspection of Figure 3. The reaction involves the movement of four electron pairs, with two separate processes which occur simultaneously (although not at the same rate): The first process, which is the more advanced in the transition state, is a nucleophilic attack of the $\pi_y(3,4)$ bond orbital to the carbonyl (C_1) carbon of ketene. The $\pi_y(3,4)$ bond orbital becomes a delocalized orbital (over C_4, C_3 and C_1) at the TS, and ends as a $\sigma(4,1)$ bond orbital of **3a**; this is of course accompanied by the conversion of the $\pi_y(1,5)$ carbon–oxygen bond of ketene into a π lone pair of oxygen, both at the TS and **3a**. The second process, which occurs mostly after the TS, is the nucleophilic attack of the $\pi_z(1,2)$ olefinic bond orbital of ketene to the C_3 of ethene, which has become electron deficient; this is readily seen at the TS, where this orbital is somewhat delocalized over C_3. The electronic deficiency thus created at C_1 is compensated by the transformation of the π_z lone pair at O_5 of ketene into the $\pi_z(1,5)$ bond orbital of cyclobutanone. Putting all these facts together, the electron pair description of the cycloaddition is schematically shown in Figure 5.

We have discussed elsewhere[26,27] how the LMO correlation analysis allows an approximate decomposition of the activation energy into bond orbital and lone pair terms. In the present case, the LMO correlation of Figure 3 shows that the breaking of the C_1–O_5 π bond makes a substantial contribution to the activation energy. In effect, both σ [$l\ \sigma(O_5)$] and π [$l\ \pi_y(O_5)$, $l\ \pi_z(O_5)$] lone pairs at oxygen are described by localized orbitals which are more energetic at the TS than at reactants or product. This is due to the increase in electron repulsion originated by the accumulation of negative charge at the oxygen atom. It is interesting to note that even the σ C_1–O_5 bond orbital, which does not "intervene" in the reaction, is destabilized at the TS relative to reactants and product. Another contributing factor to the activation energy is that the formation of the C_2C_3 bond is not accompanied by an energy decrease of

Table III. Relevant Geometrical Parameters[a,b] in the AM1 Optimized Transition States, Enthalpies of Activation[c] ($\Delta H^{\ddagger}$), and Enthalpies of Reaction[c] (ΔH_r) for the Cycloaddition of Unsymmetrically Substituted Ketenes with Ethene According to Different Approaches[d]

ketene	olefin	approach[d]	cyclobutanone	r_{12}	r_{23}	r_{34}	r_{41}	r_{15}	$\Delta H^{\ddagger}$	ΔH_r
1b	**2a**	exo	**3b**	1.384	2.476	1.397	1.752	1.222	33.7	−35.2
1b	**2a**	endo	**3b**	1.394	2.661	1.417	1.620	1.238	37.1	−35.2
1d	**2a**	exo	**3e**	1.384	2.542	1.403	1.698	1.231	37.5	−32.6
1d	**2a**	endo	**3e**	1.387	2.637	1.412	1.645	1.239	41.3	−32.6
1e	**2a**	exo	**3d**	1.398	2.535	1.389	1.776	1.225	28.0	−39.1
1e	**2a**	endo	**3d**	1.404	2.697	1.411	1.627	1.237	29.7	−39.1
1f	**2a**	exo	**3f**	1.389	2.587	1.404	1.683	1.231	36.2	−30.3
1f	**2a**	endo	**3f**	1.391	2.675	1.411	1.647	1.237	39.1	−30.3
1g	**2a**	exo	**3g**	1.390	2.589	1.405	1.682	1.232	36.1	−30.2
1g	**2a**	endo	**3g**	1.385	2.599	1.406	1.679	1.234	41.8	−30.2

[a] Atom numbering as defined in Scheme I. [b] r_{xy} are the distances in angstroms between atoms x and y. [c] At 298 K, in kcal mol^{-1}. [d] As defined in Figure 6.

the corresponding bond orbital at the TS. Thus, the tricentric $t_{1,2,3}$ orbital of the TS is not stabilized by delocalization as it could be expected (see for instance the $t_{1,3,4}$ orbital at the TS). More likely, this is due to poor overlap between the p_y atomic orbital of C_3 and the p_z atomic orbital of C_2. In fact, these orbitals are originally orthogonal in the separated fragments, and can overlap to some extent at the TS thanks to the twisting of the ethene moiety over the *xy* plane and to the incipient rotation of the ketene CH_2 group. Once the TS has been reached, the C_2–C_3 bond is formed faster than the C_1–C_4 one, as can be seen from the great decrease in orbital energy of the $t_{1,2,3}$ orbital by conversion to the $\sigma(2,3)$ bond orbital of cyclobutanone.

Turning now our attention to the cycloaddition of dichloroketene (**1c**) with ethene (**2a**), simple perturbational arguments suggest that the presence of the two chlorine atoms on the ketene moiety must provoke a significant rate enhancement of the reaction. Thus, the HOMO energy of **1c** is predicted by AM1 to be raised relative to that of **1a** by 0.17 eV, while the corresponding LUMO energy is predicted to be considerably lowered (1.07 eV). These predictions appear to be reliable, since the AM1 calculated orbital energies for **1a** and **1c** compare well with the experimentally determined ionization potentials for these species[34] via the Koopmans' theorem. Accordingly, the nucleophilic attack by the olefin on the ketene carbonyl, which as we have seen makes an important contribution to the activation energy of the reaction, should be greatly facilitated.

This is, in fact, what the results of the present study indicate (Table I), since the activation enthalpy for this reaction is calculated to be 6.7 kcal mol^{-1} lower than that of **1a** + **2a**, in full accord with the known increased reactivity of dichloroketene toward alkenes.[1e] From the geometrical point of view, the TS is very similar to that found in the cycloaddition of **1a** and **2a**, except for the C_2–C_3 bond, which is considerably elongated (Figure 2). This is probably indicative of the existence of steric repulsions between the endo chlorine atom and the proximal CH_2 group in the ethere moiety. We will see in the following sections how this kind of steric repulsions dictate the preferred interaction mode in the cycloaddition of monosubstituted ketenes with olefins.

2. Unsymmetrically Substituted Ketenes (1b,d–g) with Ethene (2a). The interaction between an unsymmetrically substituted ketene and ethene leading to [2 + 2] cycloaddition can conceivably take place in two different ways, as depicted in Figure 6.

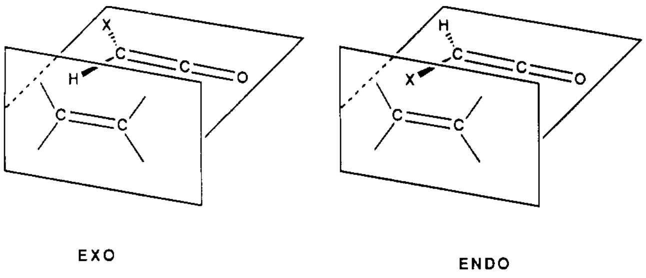

Figure 6. Schematic representation of the two possible interaction modes between an unsymmetrically substituted ketene and ethene.

In one of them, which we shall term "exo", the ethene molecule approaches to the ketene in the direction opposite to the ketene substituent. In the alternative interaction mode, to which we will refer as "endo", the olefin approach takes place through the region of space occupied by the ketene substituent. Other things being equal, it is expected that the exo approach will be favored over the endo one by steric reasons. We have located the TS's for the cycloadditions of ketenes **1b** and **1d–g** with ethene (**2a**), according to both interaction modes. The results are summarized in Table III.

As anticipated, the exo cycloadditions turn out to be in all cases the favored ones. Within this approach mode, all the considered cycloadditions are predicted to take place faster than that of the parent **1a** with ethene. The calculated order of reactivity is methoxyketene ≫ chloroketene > phenylketene ≈ vinylketene > methylketene, in good agreement with the general trends observed in the reactions of ketenes with olefins.[1] It shows also a good correlation with the calculated order of LUMO energies: chloroketene < phenylketene < methoxyketene < vinylketene < methylketene. The particular position of methoxyketene along this series appears then to indicate that the electronic requirements of the reaction can be modulated by the steric effects of the substituents. This is also evident when one compares the predicted reactivity of chloroketene with that of dichloroketene (Table I); the effect of two chlorine atoms is only somewhat larger than that of one, because of steric interactions with the olefin which will be discussed later.

From the geometrical point of view, all exo TS's are very similar to the unsubstituted one: the reactants approach to one another in a perpendicular fashion, twisted by some 50–60°, and the C_2–C_3 distance is longer than the C_1–C_4 one.

The endo approach, in turn, is characterized by more advanced transition states than the exo one. In effect, application of the bond index analysis to both interaction modes of **1b** and **2a** affords a degree of advancement of

---

[34] (a) Baker, C.; Turner, D. W. *J. Chem. Soc., Chem. Commun.* **1969**, 481. (b) Colbourne, D.; Frost, D. C.; McDowell, C. A.; Westwood, N. P. C. *J. Chem. Soc., Chem. Commun.* **1980**, 250.

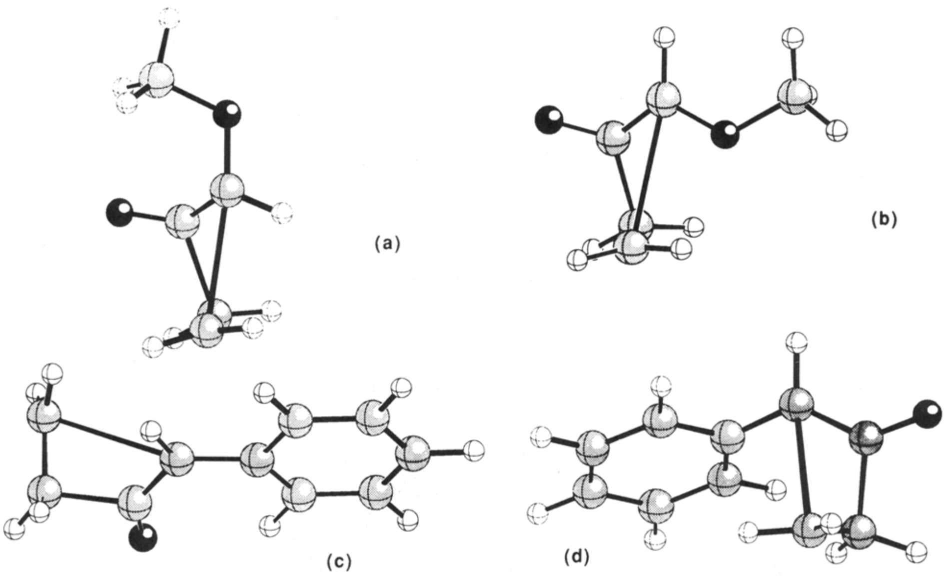

Figure 7. Computer plot of the calculated transition states for the cycloadditions of ethene (**2a**) with methoxyketene (**1e**) [(a) exo, (b) endo] and with phenylketene (**1g**) [(c) exo, (d) endo].

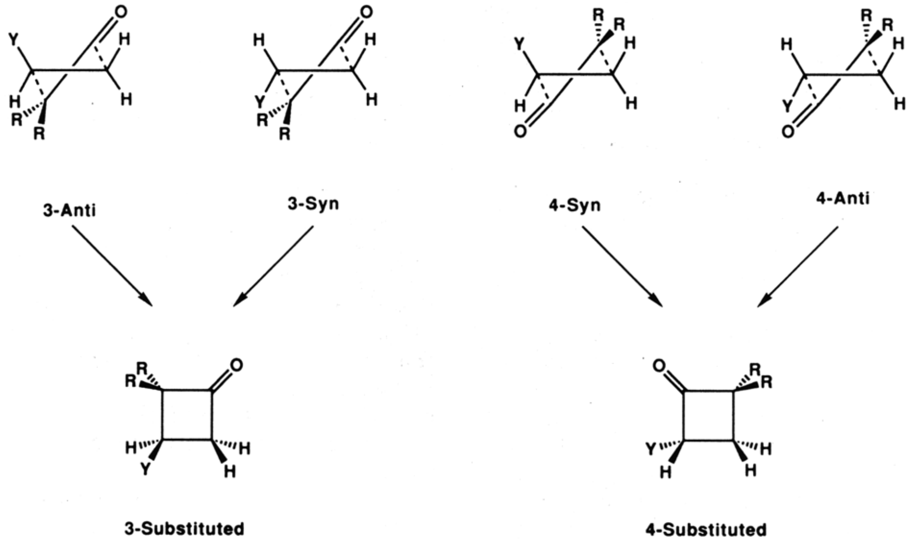

Figure 8. Schematic representation of the four possible interaction modes between a symmetrically substituted ketene and a monosubstituted olefin.

the transition state (δB_{av}) of 46.2% of the exo cycloaddition and of 56.1% for the endo one. The absolute asynchronicity (A) of the reaction, however, remains essentially the same (15.6% for the exo approach; 18.3% for the endo one). The difference between the activation enthalpies for the exo and endo approaches ($\Delta\Delta H^{\ddagger}_{endo/exo}$) ranges from 1.7 kcal mol^{-1} (**1e**) to 5.7 kcal mol^{-1} (**1g**). The order of hindrance for the endo approach is as follows: phenylketene > methylketene > chloroketene > vinylketene > methoxyketene, so that it appears to be clearly related to the steric bulk of the substituent and is in agreement with experimental facts.[35] The recorded values of $\Delta\Delta H^{\ddagger}_{endo/exo}$ help in understanding either the high reactivity of methoxyketene in the exo mode (methoxy behaves as a small substituent) or the small difference in activation energies for the cycloadditions of chloroketene and dichloroketene with ethene (the activation energy for the cycloaddition of **1c** with **2a** has a steric component of some 3.4 kcal mol^{-1}, which has to be ascribed to the repulsions between the endo chlorine atom and the ethene moiety).

From the geometrical point of view, the main characteristic of the endo TS's is that the r_{23} distances are somewhat longer and the r_{41} distances shorter than in the exo ones. The similarities and differences between exo and endo TS's can be properly appreciated in Figure 7, where the four TS's corresponding to the reactions of ethene (**2a**) with methoxyketene (**1e**) and phenylketene (**1g**) have been represented.

3. Symmetrically Substituted Ketenes (1a and 1c) with Monosubstituted Olefins (2b and 2c). These cycloadditions were selected in order to analyze the effect of olefin substitution on the rate and regioselectivity of the reaction, as well as the dependence of these effects on the simultaneous substitution of the ketene partner.

The interaction between a symmetrical ketene and a monosubstituted olefin can take place with the reactants approaching in two relative orientations, which would ultimately lead to a 3-substituted or to a 4-substituted (α-substituted) cyclobutanone. Moreover, in each orien-

---

[35] (a) Brady, W. T.; Hoff, E. F.; Roe, R.; Parry, F. H. *J. Am. Chem. Soc.* **1969**, *91*, 5679. (b) Rey, M.; Roberts, S.; Dieffenbacher, A.; Dreiding, A. S. *Helv. Chim. Acta* **1970**, *53*, 417. (c) Brady, W. T.; Roe, R. *J. Am. Chem. Soc.* **1970**, *92*, 4618. (d) Do Minh, Th.; Strausz, O. P. *J. Am. Chem. Soc.* **1970**, *92*, 1766. (e) Brady, W. T.; Roe, R. *J. Am. Chem. Soc.* **1971**, *93*, 1662. (f) Brady, W. T.; Parry, F. H.; Stockton, J. D. *J. Org. Chem.* **1971**, *36*, 1486.

Table IV. Relevant Geometrical Parameters,[a,b] Bond Indices,[c] and Enthalpies of Formation[d] for the Stationary Points in the Cycloaddition of Dichloroketene (1c) with Methyl Vinyl Ether (2c) According to the 3-Anti and the 3-Syn Approaches

approach	reaction stage	r_{12} (B_{12})	r_{23} (B_{23})	r_{34} (B_{34})	r_{41} (B_{41})	r_{51} (B_{51})	ΔH_f
3-anti	first TS	1.358 (1.485)	3.083 (0.035)	1.395 (1.365)	1.793 (0.451)	1.228 (1.745)	−21.9
	intermediate	1.379 (1.397)	2.980 (0.094)	1.434 (1.152)	1.601 (0.686)	1.248 (1.639)	−23.1
	second TS	1.396 (1.302)	2.758 (0.164)	1.449 (1.093)	1.575 (0.746)	1.247 (1.667)	−22.8
3-syn	first TS	1.357 (1.489)	3.409 (0.022)	1.398 (1.353)	1.775 (0.467)	1.230 (1.737)	−19.2
	intermediate	1.371 (1.443)	3.397 (0.032)	1.425 (1.203)	1.629 (0.633)	1.245 (1.650)	−19.7
	second TS	1.394 (1.303)	2.888 (0.166)	1.446 (1.091)	1.567 (0.763)	1.246 (1.677)	−18.4

[a] Atom numbering as defined in Scheme I. [b] r_{xy} are the distances in angstroms between atoms x and y. [c] According to eq 1, in parentheses. [d] At 298 K, in kcal mol^{-1}.

Table V. Relevant Geometrical Parameters[a,b] in the AM1 Optimized Transition States, Enthalpies of Activation[c] ($\Delta H^{\ddagger}$), and Enthalpies of Reaction[c] (ΔH_r) for the Cycloaddition of Symmetrically Substituted Ketenes with Monosubstituted Olefins According to Different Approaches[d]

ketene	olefin	approach[d]	cyclobutanone	r_{12}	r_{23}	r_{34}	r_{41}	r_{15}	$\Delta H^{\ddagger}$	ΔH_r
1a	**2b**	3-anti	**3h**	1.379	2.577	1.421	1.648	1.238	37.7	−31.5
1a	**2b**	3-syn	**3h**	1.378	2.605	1.417	1.648	1.237	38.9	−31.5
1a	**2b**	4-syn	**3e**	1.380	2.358	1.407	1.800	1.221	43.7	−31.1
1a	**2b**	4-anti	**3e**	1.379	2.385	1.409	1.781	1.223	44.5	−31.1
1a	**2c**	3-anti	**3i**	1.370	2.650	1.433	1.625	1.246	27.5	−32.6
1a	**2c**	3-syn	**3i**	1.367	2.686	1.423	1.646	1.241	30.0	−32.6
1a	**2c**	4-syn	**3d**	1.379	2.371	1.414	1.796	1.223	43.8	−31.2
1a	**2c**	4-anti	**3d**	1.379	2.406	1.417	1.766	1.225	46.3	−31.2
1c	**2b**	3-anti	**3j**	1.406	2.763	1.434	1.592	1.242	28.8	−29.8
1c	**2b**	3-syn	**3j**	1.409	2.870	1.434	1.580	1.241	30.6	−29.8
1c	**2b**	4-syn	**3k**	1.425	2.276	1.395	1.980	1.203	39.7	−30.5
1c	**2b**	4-anti	**3k**	1.417	2.336	1.397	1.927	1.206	39.3	−30.5
1c	**2c**	3-anti[e]	**3l**	1.358	3.083	1.395	1.793	1.228	17.8	−28.5
1c	**2c**	3-syn[e]	**3l**	1.394	2.888	1.446	1.567	1.246	21.3	−28.5
1c	**2c**	4-syn	**3m**	1.427	2.261	1.401	2.005	1.204	40.3	−29.8
1c	**2c**	4-anti	**3m**	1.425	2.263	1.402	2.004	1.201	40.8	−29.8

[a] Atom numbering as defined in Scheme I. [b] r_{xy} are the distances in angstroms between atoms x and y. [c] At 298 K, in kcal mol^{-1}. [d] As defined in Figure 9. [e] Highest energy transition state along the reaction path.

tation two interaction modes are possible: one in which the terminal ketene atom (i.e., C_2) approaches to the olefin from the side opposite to the substituent at C_3 (anti approach), and one in which the terminal ketene carbon approaches the olefin from the same side of the substituent (syn approach). The four possible interaction modes and the products arising therefrom are schematically represented in Figure 8.

We have studied all four possible approach geometries for the cycloadditions of **1a** and **1c** with **2b** and **2c**. The reactions have been found to be concerted in all cases but in the reactions of **1c** with **2c** leading to **3l** (3-anti and 3-syn approaches). We will discuss the nonconcerted cases first.

The relevant geometrical parameters, bond indices, and enthalpies of formation of the located stationary points in the cycloadditions of **1c** with **2c** according to the 3-anti and 3-syn approaches are summarized in Table IV.

As it can be readily seen, the interaction of **1c** with **2c** according to the 3-anti approach leads to an early TS which is the point of highest energy along the reaction path. At this stage of the reaction, most of the relevant bond indices have evolved to a comparable extent than in the concerted cases (compare with **1a** + **2a**, Table II), but the formation of the C_2–C_3 bond is hardly initiated.

Once this TS has been overcome, geometry relaxation leads to a local minimum which lies only 1.2 kcal mol^{-1} below on the potential energy hypersurface. The geometrical characteristics of this species are very similar to those of the first TS except for the C_4–C_1 bond, the formation of which has considerably progressed. The conversion of this intermediate into cyclobutanone **3l** takes place with an activation enthalpy of only 0.3 kcal mol^{-1}. Interatomic distances and bond indices in this TS are very similar to those found in analogous concerted cases (see Table V).

The intramolecular motion leading from the first to the second TS consists of a closing of the $C_4C_3C_2C_1$ dihedral angle, accompanied by a rotation of the dichloromethylene group (see Figure 9). Both movements facilitate the formation of the C_2–C_3 bond required to complete the cycloaddition.

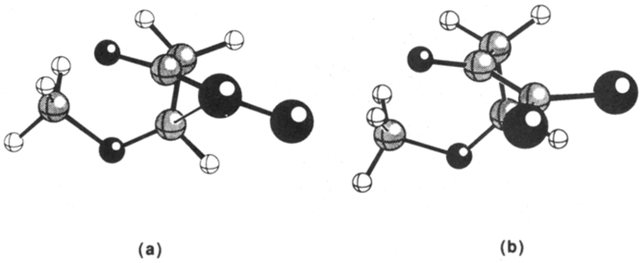

Figure 9. Computer plot of the calculated transition states for the cycloaddition of dichloroketene (**1c**) with methyl vinyl ether (**2c**) according to the 3-anti approach: (a) first TS (note that C_2 lies behind the exo chlorine atom), (b) second TS.

The alternative 3-syn approach turns out to be very similar to the 3-anti one, the main difference being that in this case the second TS is the highest energy one.

It is interesting to analyze the reasons why the mechanism of the reaction changes in these particular cases and what practical consequences, if any, can arise from this change. First of all, it is important to note that the cycloaddition of **1c** with **2c** leading to **3l** represents a limit case within the considered examples, since the best electron-donor olefin is confronted with the best electron-acceptor ketene. Moreover, **1c** represents also the situation of maximal steric bulk among the considered ketenes. As a consequence of these factors, one should expect an increased asynchronicity in the interaction between these reagents: The C_2 and C_3 atoms tend to keep away from one another in order to avoid unfavorable steric interactions, and the partial charges developed at these centers are efficiently delocalized by the respective substituents. At this point, the remaining question is whether or not these factors are sufficient to give rise to a reaction intermediate.

In fact, the region of the energy hypersurface where the located stationary points lie is very flat; the reaction intermediate for the 3-anti approach is only 0.3 kcal mol^{-1} more stable than the nearest TS, and that for the 3-syn approach is only 0.5 kcal mol^{-1} more stable than the corresponding TS. Even if these reaction intermediates had a real existence on the potential energy hypersurface, no stereochemical consequences (for instance, when chiral enol ethers participate in the reaction[3]) ought to be expected, i.e., rotation around the C_3–C_4 bond would be much more energy consuming than reaction completion. On the other hand, due to the very similar values of the enthalpies of formation of the different stationary points, an incorrect description of this region of the potential energy hypersurface by AM1 cannot be completely ruled out. In summary, the cycloadditions of **1c** with **2c** according to the 3-anti and the 3-syn approaches can probably be considered as borderline two-stage concerted reactions rather than genuine stepwise processes.

We will discuss now the more general concerted cases. The relevant geometrical parameters of the located transition states are summarized in Table V along with the activation enthalpies of the corresponding cycloadditions. Information on the highest energy TS's in the already discussed "nonconcerted" cases are also included for comparison.

From the experimental point of view, it is well known that the cycloadditions of ketenes with substituted olefins are highly regioselective, leading to 3-substituted cyclobutanones.[1] The first important point to be noted is that AM1 correctly reproduces this behavior, since 3-substituted cyclobutanones are predicted to be in all cases the exclusive products of the cycloadditions.

Among the processes leading to 3-substituted products, the 3-anti approach turns out to be the favored one. This is, consequently, the predicted reaction mode of symmetrically substituted ketenes with monosubstituted olefins.

The predicted order of reactivity of olefins toward ketene is methyl vinyl ether ≫ propene > ethene. Moreover, dichloroketene is predicted to be much more reactive than the parent ketene toward any particular olefin. Both predictions are in full agreement with the known experimental facts.[1] Bearing in mind the mechanistic picture of the reaction discussed above, the facts which are relevant to this order of reactivity are the energies of the HOMO of the olefins (**2c**, –9.41 eV; **2b**, –9.99 eV; **2a**, –10.55 eV) and of the LUMO of the ketenes (**1c**, –0.73 eV; **1a**, 0.34 eV), which facilitates the nucleophilic attack on the ketene and, more importantly, the stabilization of the TS by the substituents of the reactants. Thus, the electron deficiency created at C_3 in the TS is partially compensated by conjugation with an oxygen lone pair (**2c**) or by hyperconjugation (**2b**), whereas the excess electron density at C_2 can be efficiently delocalized by the electronegative chlorine atoms of **1c**.

The complementary 3-syn approach is characterized by slightly higher activation enthalpies, mainly reflecting the additional steric interactions associated with bringing the ketene and olefin substituents into closer proximity.

Turning now our attention to the higher energy approach leading to the α-methyl- and α-methoxycyclobutanones **3d**, **3e**, **3k**, and **3m**, it is important to note that in this case the preferred interaction mode is—except for **1c** + **2b**—the 4-syn one, and this probably happens because in this way the steric crowding between the ketene oxygen and the substituent of the olefin (at C_4) is minimal.

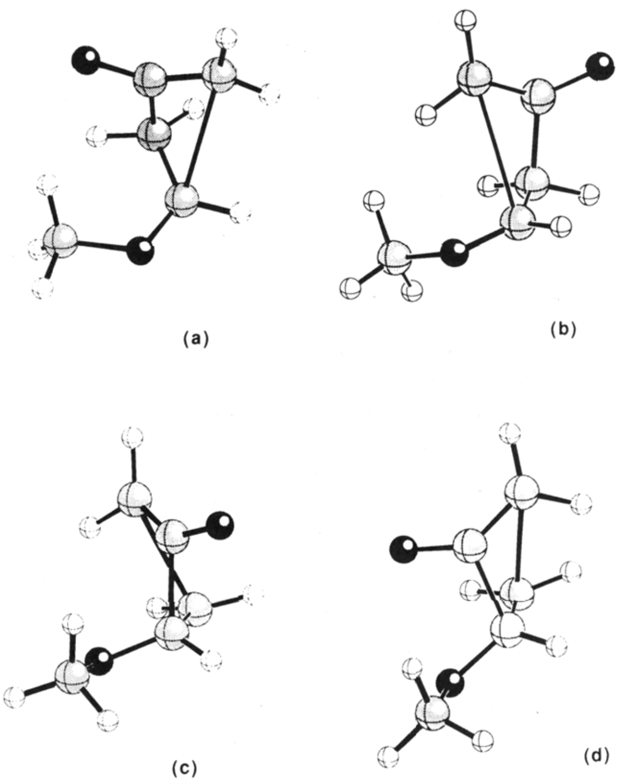

Figure 10. Computer plot of the calculated transition states for the cycloaddition of ketene (**1a**) with methyl vinyl ether (**2c**): (a) 3-anti, (b) 3-syn, (c) 4-syn, (d) 4-anti.

The difference in activation enthalpies between the 4-syn and the 3-anti approaches ($\Delta\Delta H^{\ddagger}_{\text{4-syn/3-anti}}$) is then responsible for the regioselectivity of these cycloadditions. Inspection of the data in Table V clearly shows the electronic origin of this term: The presence of a methyl substituent on the olefin introduces a difference of ca. 6 kcal mol^{-1} between both reaction modes as a consequence of the loss of hyperconjugation stabilization in the 4-syn TS. When the olefin substituent is methoxy, the difference is much larger (ca. 16 kcal mol^{-1}), thus reflecting the important conjugative stabilization of the corresponding 3-anti TS, which is completely absent from the 4-syn one. When the *gem*-dichloro substituent is present on the ketene, these figures are increased in some 5–6 kcal mol^{-1}, in spite of the additional steric interactions present in the 3-anti TS's.

From the geometrical point of view, the located TS's do not differ substantially from those already discussed. In general, the TS's corresponding to the syn and anti approaches leading to the same regioisomer are very similar in their ring parameters, and the processes leading to α-substituted cyclobutanones are characterized by a somewhat more synchronous formation of the C_2–C_3 and C_4–C_1 bonds. We have represented in Figure 10 all four TS's for the cycloaddition between ketene (**1a**) and methyl vinyl ether (**2c**). Note that in these TS's the conformation of the methoxy group is very different, since it is eclipsed in the 3-anti and 3-syn approaches and extended in the 4-syn and 4-anti ones. The conformational preference of the methoxy group appears to be fairly constant in the studied cases, and amounts to ca. 4 kcal mol^{-1} for the 3-anti approach and to ca. 2 kcal mol^{-1} for the 4-syn approach. This last point should be helpful in the interpretation of the face selectivities observed in the asymmetric cycloadditions between ketenes and enol ethers.[3]

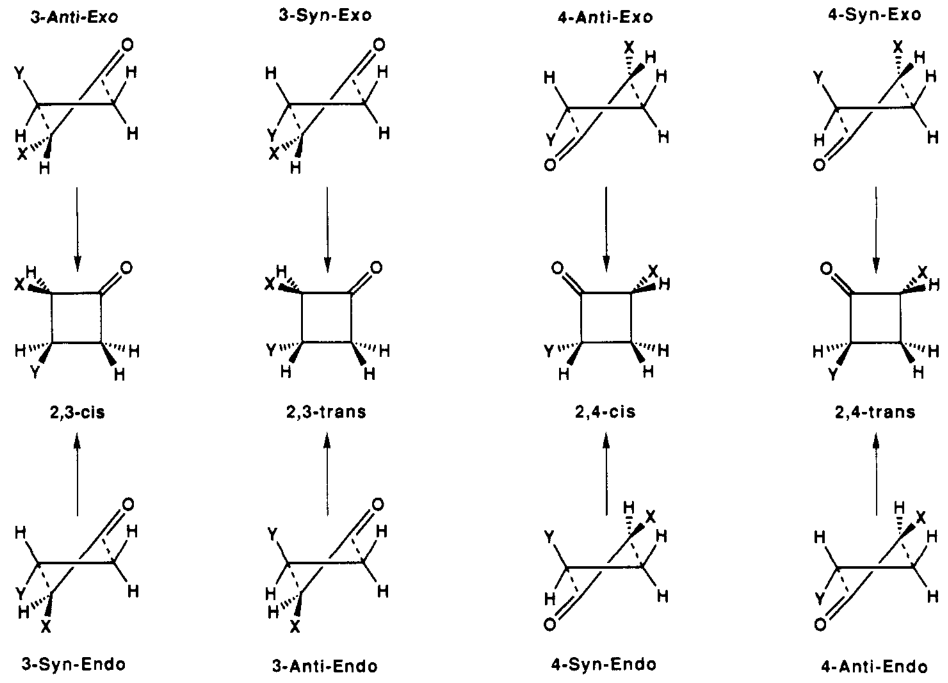

Figure 11. Schematic representation of the eight possible interaction modes between a monosubstituted ketene and a monosubstituted olefin.

4. Monosubstituted Ketenes (1b and 1d) with Monosubstituted Olefins (2b and 2c). The study of these cycloadditions was undertaken in order to investigate the most interesting stereochemical feature of the reaction, i.e. the fact that the resulting cyclobutanone always has the bulkiest ketene and olefin substituents in a 1,2-cis relative arrangement. This phenomenon has been mostly studied in the cycloadditions of cyclopentadiene with a variety of monosubstituted and unsymmetrically disubstituted ketenes, where it results in a preference of the bulkiest ketene substituent for the endo stereochemistry,[35] and has been called a *masochistic steric effect.*

The interaction between a monosubstituted ketene and a monosubstituted olefin can take place in eight different ways as a result of regiochemical and stereochemical variations (Figure 11).

As it can be readily appreciated, any of the four possible products can arise from two different interaction modes. Bearing in mind the results that we have already discussed, it can be anticipated that 2,3-cis-disubstituted cyclobutanones will be preferentially formed through a 3-anti-exo TS, and that the corresponding 2,4-trans-disubstituted cyclobutanones will arise from a 4-syn-exo approach, since these reaction modes appear to be essentially free of steric interactions.

In the formation of the diastereomeric 2,3-trans-disubstituted and 2,4-cis-disubstituted derivatives, however, both interaction modes should be in principle considered. In one of the approaches leading to these substances the exo preference of the ketene substituent is preserved, whereas in the other one the olefin substituent is in the most sterically free arrangement. As we have seen in the second section of this discussion, the preference of exo arrangement in the cycloadditions of chloroketene (1b) and methylketene (1d) with ethene (2a) amounts to 3.4 and 3.8 kcal mol^{-1}, respectively. On the other hand, the results in the third section of this discussion show that the preference of methyl vinyl ether (2c) for the most sterically free arrangement in the cycloaddition with ketene (1a) amounts to 2.5 kcal mol^{-1}, irrespective of the regioisomer formed in the reaction. In the case of propene (2b), this preference is much smaller (0.8–1.2 kcal mol^{-1}). Accordingly, in order to ensure the study of the lowest energy reaction paths leading to any of the four possible disubstituted cyclobutanones under consideration, we have studied all possible exo approaches for the cycloadditions of 1b and 1d with 2b and 2c, plus the 3-anti-endo and the 4-syn-endo modes for the reactions of 1b and 1d with 2c. The results are summarized in Table VI.

As it can be readily seen, the preferred interaction mode is in all cases the 3-anti-exo one, which leads to cis-2,3-disubstituted cyclobutanones. Thus, AM1 correctly reproduces the regio- and stereochemical outcome of the cycloadditions of substituted ketenes with substituted olefins. According to the results in the previous sections, the preference for the formation of the cis-2,3-disubstituted products appears to be the result of two contributing factors: an electronic preference for the formation of 3-substituted cycloadducts and a steric preference for the anti-exo interaction mode. Within this approach, the reaction is predicted to proceed in all cases faster than that of ketene (1a) with ethene (2a); moreover, the effect of all the considered substituents turns out to be very nearly additive, i.e., the $\Delta H^{\ddagger}$ values for the different cycloadditions can be accurately estimated from the activation enthalpy of the parent cycloaddition and the substituent effects deduced from the results in Sections 2 and 3. [For ketene substituents: chloro, −6.1 kcal mol^{-1}; methyl, −2.3 kcal mol^{-1}. For olefin substituents: methyl, −2.1 kcal mol^{-1}; methoxy, −12.3 kcal mol^{-1}.]

As a general trend, the next most favorable approach is the 3-syn-exo one, which leads to 2,3-trans-disubstituted cyclobutanones. However, when 2c is involved in the reactions, the 3-anti-endo approach, which leads to the same compounds, turns out to be more favorable. It is important to realize that the conformational preferences of the methoxy group are larger, in energy terms, than the recorded differences between the 3-anti-exo, 3-syn-exo, and 3-anti-endo approaches. Thus, in the 3-anti-exo and 3-anti-endo modes, the preference of the methoxy group for the eclipsed conformation amounts to ca. 4.0 kcal mol^{-1}. One the other hand, in the 3-syn-exo approach the preference for the eclipsed conformation is much weaker, amounting only to ca. 0.5 kcal mol^{-1}. It is thus expected

Table VI. Relevant Geometrical Parameters[a,b] in the AM1 Optimized Transition States, Enthalpies of Activation[c] ($\Delta H^{\ddagger}$), and Enthalpies of Reaction[c] (ΔH_r) for the Cycloaddition of Monosubstituted Ketenes with Monosubstituted Olefins According to Different Approaches[d]

ketene	olefin	approch[d]	cyclobutanone	r_{12}	r_{23}	r_{34}	r_{41}	r_{15}	$\Delta H^{\ddagger}$	ΔH_r
1b	**2b**	3-anti-exo	**3n**	1.381	2.638	1.413	1.672	1.233	31.4	−30.3
1b	**2b**	3-syn-exo	**3r**	1.382	2.665	1.410	1.670	1.232	32.6	−31.5
1b	**2b**	4-syn-exo	**3z**	1.399	2.208	1.402	1.958	1.205	37.3	−31.0
1b	**2b**	4-anti-exo	**3v**	1.395	2.283	1.402	1.896	1.210	38.1	−30.9
1b	**2c**	3-anti-exo	**3p**	1.363	2.813	1.413	1.692	1.236	21.5	−30.4
1b	**2c**	3-syn-exo	**3t**	1.364	2.806	1.409	1.704	1.232	24.3	−32.7
1b	**2c**	3-anti-endo	**3t**	1.392	2.648	1.454	1.568	1.249	21.7	−32.7
1b	**2c**	4-syn-exo	**3ab**	1.397	2.256	1.408	1.921	1.210	37.2	−31.0
1b	**2c**	4-anti-exo	**3x**	1.391	2.358	1.411	1.834	1.216	40.1	−30.1
1b	**2c**	4-syn-endo	**3x**	1.390	2.641	1.424	1.656	1.239	44.2	−30.1
1d	**2b**	3-anti-exo	**3o**	1.385	2.647	1.420	1.642	1.240	35.2	−27.7
1d	**2b**	3-syn-exo	**3s**	1.385	2.677	1.416	1.639	1.238	36.4	−28.8
1d	**2b**	4-syn-exo	**3aa**	1.385	2.440	1.406	1.764	1.226	41.7	−28.4
1d	**2b**	4-anti-exo	**3w**	1.394	2.223	1.404	1.947	1.209	43.3	−28.4
1d	**2c**	3-anti-exo	**3q**	1.372	2.747	1.425	1.639	1.245	25.7	−28.7
1d	**2c**	3-syn-exo	**3u**	1.369	2.785	1.416	1.666	1.239	28.3	−29.5
1d	**2c**	3-anti-endo	**3u**	1.385	2.690	1.445	1.585	1.251	28.1	−29.5
1d	**2c**	4-syn-exo	**3ac**	1.385	2.453	1.413	1.761	1.228	41.6	−28.5
1d	**2c**	4-anti-exo	**3y**	1.391	2.290	1.411	1.896	1.214	44.7	−28.4
1d	**2c**	4-syn-endo	**3y**	1.383	2.493	1.413	1.763	1.231	46.9	−28.4

[a] Atom numbering as defined in Scheme I. [b] r_{xy} are the distances in angstroms between atoms x and y. [c] At 298 K, in kcal mol^{-1}. [d] As defined in Figure 11.

that in cycloadditions of enol ethers containing alkoxy groups bulkier than methoxy, the eclipsed arrangement of the alkoxy group will become less favorable and, hence, the 3-anti-endo approach will be destabilized relative to the 3-syn-exo one.

The reaction modes leading to 2,4-disubstituted cyclobutanones are characterized by much more energetic TS's, thus justifying the very high regioselectivity depicted by these cycloadditions. The most favorable approach turns out to be the 4-syn-exo one, which is essentially free of steric interactions between the ketene and olefin substituents and leads to 2,4-trans-disubstituted cyclobutanones. If one compares the 3-anti-exo and the 4-syn-exo approaches term by term, the differences in $\Delta H^{\ddagger}$ reflect the loss of conjugative or hyperconjugative stabilization in the TS's leading to the 2,4-regioisomers. As already discussed in Section 2, these differences depend only on the olefin involved in the reaction, and amount to ca. 6 kcal mol^{-1} for propene and to ca. 16 kcal mol^{-1} for methyl vinyl ether. Within the 4-syn-exo approach, the $\Delta H^{\ddagger}$ values depend only on the ketene involved in the reaction, being 4.4 kcal mol^{-1} higher for methylketene (**1d**).

The alternative 4-anti-exo interaction, which leads to 2,4-cis-disubstituted cyclobutanones, is characterized by somewhat more energetic TS's as a consequence of the additional steric interaction between the olefin substituent and the ketene carbonyl. In this case, the complementary 4-syn-endo approach, investigated for the cycloadditions of **1b** and **1d** with methyl vinyl ether, show activation enthalpies higher than the 4-anti-exo one.

From the geometrical point of view, the calculated TS's are similar to that of the parent process. As a general trend, the processes leading to the 2,4-regioisomers take place through somewhat more synchronous TS's, as it was already observed in the cycloadditions of monosubstituted olefins with symmetrically substituted ketenes discussed in Section 3. We have represented in Figure 12 the transition states corresponding to the most favorable formation of the four possible products of the cycloaddition between chloroketene (**1b**) and methyl vinyl ether (**2c**).

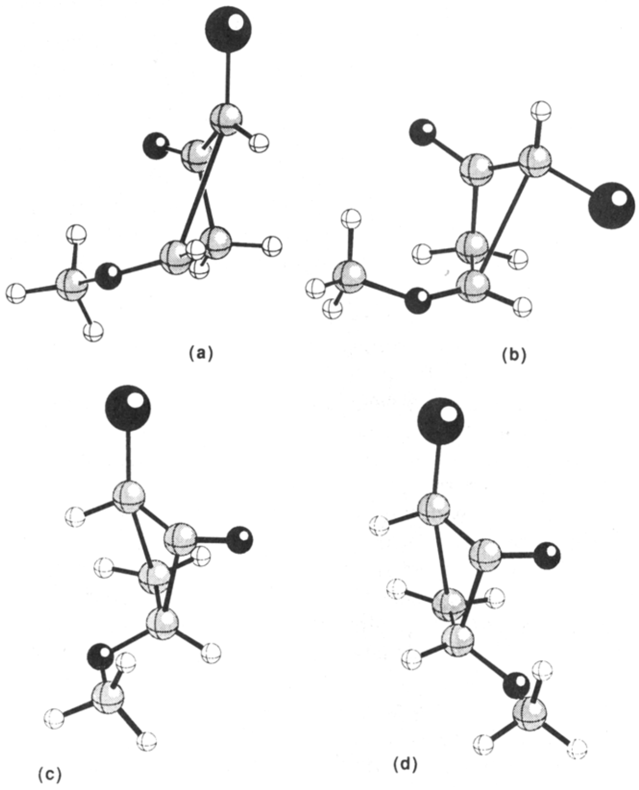

Figure 12. Computer plot of the most favorable calculated transition states for the cycloaddition of chloroketene (**1b**) with methyl vinyl ether (**2c**): (a) 3-anti-exo, (b) 3-anti-endo, (c) 4-syn-exo, (d) 4-anti-exo.

Conclusions

The following conclusions can be drawn from the present study:

(1) The semiempirical SCF MO method AM1 predicts that the cycloaddition of ketenes with olefins takes place in a concerted but nonsynchronous manner, through twisted transition states with small charge separation in which the formation of the new bond involving the ketene carbonyl group is already advanced. This is in full agreement with the accepted mechanistic picture of the reaction arising from experimental studies.

(2) A correlation analysis of localized molecular orbitals for the cycloaddition of ketene with ethene reveals that the reaction mechanism fits well with the $[_{\pi}2_s + (_{\pi}2_s + _{\pi}2_s)]$

description, though four electron pairs, rather than three, participate in the process.

(3) The very high regioselectivity usually depicted by these cycloadditions appears to obey electronic reasons, i.e., to the conjugative or hyperconjugative stabilization of the transition state leading to the observed regioisomer by the olefin substituent.

(4) The striking diastereoselectivity of this reaction is well reproduced by the calculations, and it is seen to obey the minimization of steric interactions between the substituents of the ketene and olefin partners in the transition state.

(5) The calculated substituent effects on reaction rates, regioselectivities, and stereoselectivities are in good agreement with the available experimental results.

Acknowledgment. The calculations were performed with the IBM 3090 computer at the "Centre d'Informàtica de la Universitat de Barcelona". Financial support from the CICYT (Grant PB86-510) is gratefully acknowledged. We are indebted to Dr. Josep M. Bofill for making available to us the program for TCSCF calculations. We also thank Prof. Santiago Olivella and Dr. Antoni Riera for helpful discussions.

Supplementary Material Available: Cartesian coordinates of the optimized molecular structures (67 pages). Ordering information is given on any current masthead page.

Heats of Reaction for Nucleophilic and Electrophilic Displacement Reactions in Solution

Edward M. Arnett,* Kalyani Amarnath, and Sampath Venimadhavan

Department of Chemistry, Duke University, Durham, North Carolina 27706

Received November 30, 1989

Measured heats of displacement, ΔH_{dis}, in sulfolane/3-methylsulfolane solution at 25 °C, are reported for the attack of carbenium ions and various anions on neutral compounds, most of whose heats of heterolysis, ΔH_{het}, have been published previously. Some new ΔH_{het} values are derived from measured heats of reaction of resonance-stabilized carbenium ions with inorganic anions. In most cases there is good agreement between the measured ΔH_{dis} and that calculated by the First Law from the combined ΔH_{het}s. However, large discrepancies are found for other cases, and these are shown to be due to formation of a variety of products, presumably because of extreme steric hindrance to direct displacement at the original bonding site.

Introduction

Nucleophilic and electrophilic displacements encompass a major domain of mechanistic study.[1] Historically, they have been approached primarily in terms of kinetics with relatively little consideration of the overall thermodynamics of such processes. Against this background, results reported here are, to the best of our knowledge, the first thermochemical data available for the heats of nucleophilic displacement of one base by another, or electrophilic displacement of one carbenium ion by another from neutral compounds.

Recently we became engaged in an extensive investigation of direct reactions between carbenium ions with a wide variety of anionic bases. The kinetics, thermodynamics, and electrochemistry for such systems, including the energetics of bond cleavage to form ions or radicals, were reported.[2-6] Heats of reaction (rxn) for the coordination (coord) of carbenium ions with carbanions to form neutral species led to an extensive tabulation[7-11] of heterolysis (het) energies (Scheme I) and these values were correlated with remarkably high precision to the pK_as of the conjugate acids[12] of the carbanions and the pK_{R^+}s of the carbenium ions.[13] With this information in hand it is reasonable to predict that highly reactive anions which form a strong bond (high ΔH_{het}) with a given carbenium ion should displace more stable anions which form less endothermic bonds. Exactly the same reasoning applies to displacement reactions by carbenium ions. By means of the First Law, the heats of displacement should be accurately predictable as the difference between the heats of heterolysis of the bond being broken and the bond being made. This article describes the application of this simple proposal to displacement reactions.

Scheme I

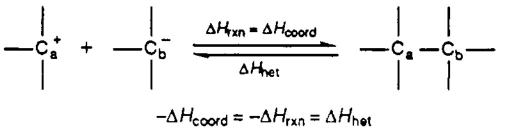

Until this point, our research has been limited to resonance-stabilized organic anions. However, extensive kinetic studies of carbenium ions with inorganic anions in predominantly aqueous solution by Ritchie and others[14,15]

---

(1) (a) Lowry, T. H.; Richardson, K. S. *Mechanisms and Theory in Organic Chemistry*, 3rd ed.; Harper & Row: New York, 1987. (b) March, J. *Advanced Organic Chemistry*, 3rd ed.; John Wiley & Sons: New York, 1985. (c) Harris, J. M.; McManus, S. P., Eds. *Nucleophilicity*; Advances in Chemistry Series; American Chemical Society: Washington, DC, 1987.

(2) Arnett, E. M.; Troughton, E. B. *Tetrahedron Lett.* **1983**, *24*, 3299.

(3) Arnett, E. M.; Troughton, E. B.; McPhail, A.; Molter, K. E. *J. Am. Chem. Soc.* **1983**, *105*, 6172.

(4) Troughton, E. B.; Molter, K. E.; Arnett, E. M. *J. Am. Chem. Soc.* **1984**, *106*, 6726.

(5) Arnett, E. M.; Molter, K. E. *J. Phys. Chem.* **1986**, *90*, 471.

(6) Arnett, E. M.; Molter, K. E. *Acc. Chem. Res.* **1985**, *18*, 339.

(7) Arnett, E. M.; Chawla, B.; Molter, K. E.; Amarnath, K.; Healy, M. *J. Am. Chem. Soc.* **1985**, *107*, 5288.

(8) Arnett, E. M.; Chawla, B.; Amarnath, K.; Whitesell, L. G., Jr. *Fuel Energy* **1987**, *1*, 17.

(9) Arnett, E. M.; Whitesell, L. G., Jr.; Amarnath, K.; Cheng, J.-P.; Marchot, E. *Die Macromolekular Chemie*; Macromolecular Symposium (Munich, 1987) **1988**, *13/14*, 21-31.

(10) Arnett, E. M.; Harvey, N. G.; Amarnath, K.; Cheng, J.-P. *J. Am. Chem. Soc.* **1989**, *111*, 4143.

(11) Arnett, E. M.; Amarnath, K.; Harvey, N. G.; Cheng, J.-P. *J. Am. Chem. Soc.* **1990**, *112*, 344.

(12) Bordwell, F. G. *Acc. Chem. Res.* **1988**, *21*, 456 and private communications.

(13) Bethell, D.; Gold, V. In *Carbonium Ions*; Academic Press: New York, 1967.

(14) Ritchie, C. D. *Can. J. Chem.* **1986**, *64*, 2239.

(15) McClelland, R. A.; Banait, N.; Steenken, S. *J. Am. Chem. Soc.* **1989**, *111*, 2929.

0022-3263/90/1955-3593$02.50/0